



RESEARCH ARTICLE

Turnover of soil microaggregate-protected carbon and the challenge of microscale analyses

Nele Meyer^{1,2} | Jacqueline Kaldun¹ | Andrei Rodionov¹ | Wulf Amelung³ | Eva Lehndorff¹

¹Department of Soil Ecology, University of Bayreuth, Bayreuth, Germany

²Institute of Physical Geography, Goethe University Frankfurt, Frankfurt, Germany

³Institute of Crop Science and Resource Conservation, Soil Science and Soil Ecology, University of Bonn, Bonn, Germany

Correspondence

Nele Meyer, Institute of Physical Geography, Goethe University Frankfurt, Altenhöferallee 1, 60438 Frankfurt, Germany.
Email: nele.meyer@em.uni-frankfurt.de

This article has been edited by Kai Uwe Totsche.

Funding information

German Research Foundation, Grant/Award Numbers: DFG Am 134/25/2, 251268514

Abstract

Background: Microaggregates are suspected to protect soil organic carbon (SOC) from microbial decay, but its residence time is not well understood.

Aims: We aimed at unraveling the relevance of microaggregates for C storage and testing the hypothesis that C in the interior of aggregates is older, compared to the exterior.

Methods: We sampled soil under C3 vegetation and at a site where cropping shifted to C4 vegetation 36 years ago. We isolated free and macroaggregate-occluded size fractions (250–53 μm) by wet sieving and ultrasound, manually isolated aggregates therefrom, and analyzed whether vegetation-related differences in $\delta^{13}\text{C}$ could be traced at the interior and exterior of microaggregate cross-sections using elemental and laser ablation-isotope ratio mass spectrometry.

Results: Size fraction weights comprised <5% of microaggregates. Based on a source partitioning approach including C3- and C4-derived C, we found mean residence times of SOC in occluded and free microaggregates of 62 and 105 years, respectively. Thus, C storage was longer than that in size fractions (35 years) and bulk soil (58 years). The small-scale variability of $\delta^{13}\text{C}$ within aggregate cross-sections was considerable, both in C3 and C4 soil, yet without significant ($p = 0.46$) differences between interior and exterior locations.

Conclusions: We conclude that microaggregates do not persist in an intact form in such a long-term that systematic differences in $\delta^{13}\text{C}$ patterns between exterior and interior parts can develop.

KEYWORDS

carbon stabilization, laser-ablation isotope ratio mass spectrometry, mean residence time, stable isotope mixing

1 | INTRODUCTION

The mean residence time (MRT) of different soil organic matter (SOM) constituents ranges from days to millennia (e.g., Derrien & Amelung, 2011; Flessa et al., 2008; Gleixner et al., 2002; Jenkinson, 1990). The

long-term stability of SOM is controlled by stabilization mechanisms, among which physical stabilization through microaggregate (<250 μm) formation is considered to be critically important (Foster, 1988; Ladd et al., 1993; Six et al., 2004). Microaggregates form through various physical, chemical, and biological interactions that induce a binding of

This is an open access article under the terms of the [Creative Commons Attribution](https://creativecommons.org/licenses/by/4.0/) License, which permits use, distribution and reproduction in any medium, provided the original work is properly cited.

© 2024 The Authors. *Journal of Plant Nutrition and Soil Science* published by Wiley-VCH GmbH.

primary particles, organic matter, and microbial residues to stable units that can withstand mechanical stress and protect SOM from decomposition (Totsche et al., 2018). Microaggregates may be further occluded within macroaggregates larger than 250 μm (Six et al., 2004). Although macroaggregates have been considered less stable than microaggregates (Elliott, 1986; Totsche et al., 2018; Waters & Oades, 1991), they may provide additional protection of occluded microaggregates and increase the MRT of soil organic carbon (SOC) stored therein (Buyanovsky et al., 1994; Six et al., 2004). Estimates of the MRT of SOC in large microaggregates range between 60 years in a Stagnic Luvisol (54 years in bulk soil; John et al., 2005), 61 years in a Gleysol (14 years in macroaggregates; Monreal et al., 1997), 310 years in an Alfisol (300 years in macroaggregates; Rabbi et al., 2013), and 265–504 years in an Oxisol (320–485 years in macroaggregates; Rabbi et al., 2013).

On a small spatial scale of individual aggregates, the MRT may vary along a gradient from the aggregate's surface (i.e., exterior) to the center (i.e., interior). Some earlier work suggested an inclusion of microbial-derived C as an organic core inside microaggregates (Foster, 1988; Ladd et al., 1993). Other researchers suspect particulate organic matter (POM) to serve as a nucleus for aggregate formation (Bucka et al., 2019; Jastrow, 1996). These studies suggest a different contribution of building units along a gradient from the aggregate's exterior to the interior. Yet, Lehndorff et al. (2021) failed to detect a systematic enrichment of SOC within the center of a microaggregate cross-section. Nevertheless, oxygen diffusion inside aggregates is likely restricted (Sexstone et al., 1985), which may result in low microbial activity and consequent protection of SOC at the interior of aggregates. Hence, SOC at the interior of aggregates is likely physically protected from decay (Amelung & Zech, 1996), also allowing SOC at the interior of microaggregates to age. In contrast, microbial activity at the accessible exterior of aggregates may leave behind rather young SOC, from microbial biomass and its residues.

For estimating the turnover of bulk SOC and individual organic compounds, C3/C4 vegetation change experiments have been widely used (Amelung et al., 2008; Balesdent et al., 1998; Schiedung et al., 2017). Such approaches have mainly been used to study the MRT of C in aggregate fractions or bulk soil. Yet, information on the small-scale spatial arrangement of young (i.e., C4-derived) and old (i.e., C3-derived) SOC in soil is still lacking. Hence, it has to our knowledge not been studied yet whether SOC stored at the interior of microaggregates is older than SOC stored at the exterior. Novel techniques such as laser ablation-isotope ratio mass spectrometry (LA-IRMS) allow to zoom into microscale soil structures and investigate the spatial pattern of C turnover via $\delta^{13}\text{C}$ analyses (Rodionov et al., 2019), and thus also along cross-sections of individual macroaggregates (Vergara Sosa et al., 2021). The technique should thus also be suitable to study small-scale patterns of $\delta^{13}\text{C}$ within microaggregates in combination with a C3/C4 vegetation change experiment allowing to attribute SOC to its source, that is, to localize old C3-SOM and young C4-SOM within individual aggregates. The stable C isotope composition of SOC is driven by two major mechanisms: mixing of C from different sources such as C3 and C4 vegetation (Amelung et al., 2008; Balesdent & Mariotti, 1996) and isotope fractionation mainly caused by preferential metabolization of

“light” molecules during microbial decomposition of SOM (Fernandez et al., 2003; Gleixner et al., 1993; Krüger et al., 2023). The latter does usually not complicate source partitioning approaches when suitable controls from C3 soil with a similar magnitude of fractionation processes exist. Whether this becomes an issue in small-scale approaches is still uncertain.

Besides the potential of aggregates to stabilize SOC, their quantitative relevance for C storage is still in debate. Depending on the reference soil group under consideration, some studies consider aggregates to be of minor quantitative relevance (e.g., Burger et al., 2023; Krause et al., 2018), while others fractionate the total soil mass into several conceptually defined aggregate size classes, implying that their sum is 100% (Jiang et al., 2011; Shrestha et al., 2004). In this context, and apart from soil texture, a major reason for this knowledge gap relates to the aggregate fractionation procedure. Most studies are based on measurements of size fractions obtained after wet- or dry-sieving with or without additional sonication to release microaggregates occluded in macroaggregates (e.g., Jiang et al., 2011; Shrestha et al., 2004). However, such fractionation approaches do not isolate pure aggregates but fractions that additionally contain free POM and mineral particles (Moni et al., 2012; Poeplau et al., 2018). The presence of mineral components may lead to an overestimation of the quantitative importance of aggregates, especially in cases where no sand correction has been performed (Elliott et al., 1991). Likewise, the presence of typically young POM may lead to underestimation of the MRT of aggregates when ^{13}C measurements are performed on fractions but not on isolated aggregates.

In this study, we analyzed $\delta^{13}\text{C}$ natural abundance in soil, size fractions, and therefrom isolated microaggregates following a C3/C4 vegetation change at Rotthalmünster, Germany. We also investigated spatial gradients of $\delta^{13}\text{C}$ inside individual microaggregates. We assumed that microaggregates contain a larger percentage of “old” SOC than bulk soil or size fractions, that is, SOC originating from C3 vegetation prior to changes to C4 cropping. Old SOC will be preferentially allocated at the interior of microaggregates due to physical protection. The results will provide new insights into aggregate formation and disruption processes and associated C turnover in soil.

2 | MATERIAL AND METHODS

2.1 | Study site and soil sampling

Soil was collected in December 2015 from the Ap horizon (5–20-cm depth) of a loess-derived Stagnic Luvisol in Rotthalmünster (Germany, 48°21'47''N, 13°11'46''E, elevation: 360 m asl), which has been under continuous maize cropping since 1979, that is, 36 years before sampling. The field trial is in detail described in John et al. (2005) and Flessa et al. (2008). The soil texture is a silt loam (11% sand, 73% silt, 16% clay; Flessa et al., 2008). Adjacent soil, which was under C3 vegetation cropping (wheat since 1969) was taken as control. Five replicates were collected from randomly selected spots on both sites using soil cylinders with a volume of 3 L and a height of 15 cm. Fresh samples were

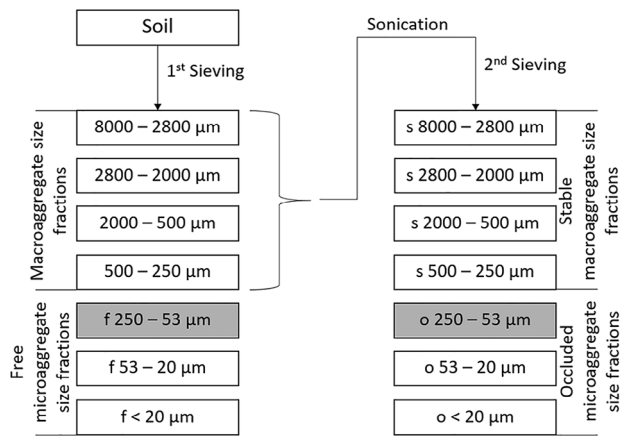


FIGURE 1 Soil fractionation scheme. In this study, we focused on aggregate size fractions highlighted in gray.

immediately sieved to <8 mm and stored at 4°C until fractionation. We refer to the C3/C4 vegetation change soil as “C4 soil” and to the control soil as “C3 soil” throughout the article.

2.2 | Aggregate fractionation

We performed a size fractionation in line with Elliott (1986) as outlined in detail in Lobe et al. (2011) and presented in Figure 1. In brief, 50 g of soil was carefully wetted and slaked for 5 min. An electrically driven sieve tower, including five sieves (2800, 2000, 500, 250, 53 μm), moved 300 times up and down within 10 min with a vertical movement of 3 cm. The material remaining on each sieve was collected, and the remnant was sieved through a 20- μm sieve. The solution that passed the 20- μm sieve was collected, and particles were precipitated by adding MgCl_2 . Hence, seven water stable aggregate classes were separated, including macroaggregates (8000–2800, 2800–2000, 2000–500, and 500–250 μm) and free microaggregates (f250–53, f53–20, and <20 - μm fraction). For subsequent fractionation of occluded microaggregates, macroaggregates >250 μm were sonicated at an energy output of 60 J mL^{-1} , and sieving was repeated as described above. In this second step, three classes of occluded microaggregates were separated (o250–53, o53–20, and o < 20 - μm fraction), though this procedure also yielded some infrequently resisting “stable” macroaggregates (s8000–2800, s2800–2000, s2000–500, and s500–250 μm). Directly after aggregate-size fractionation, all aggregate classes were shock-frozen using liquid nitrogen and freeze-dried for minimizing alterations of microaggregate properties during drying (Siebers et al., 2018). According to Siebers et al. (2018), freeze-drying only slightly alters the morphology of the aggregates but prevents severe decomposition and re-aggregation processes as observed with other drying methods. The dried fractions were weighed to quantify their proportion to the soil.

In this study, we only focus on free and occluded large microaggregates in the size fraction 250–53 μm . The smaller fractions were not

considered, as they were too small for manual isolation, and the larger fractions were excluded as macroaggregates were not the scope of this study.

The obtained 250–53 μm fractions (Figure 1) contained besides aggregates considerable proportions of free minerals and POM (Figure 2a). Thus, we quantified the weight proportion of 250–53-sized aggregates in the free and occluded size fraction. Under a stereomicroscope, such aggregates were easily recognizable by the typical round or oval shape and dark color (Figure 2b). Additional investigation using a raster electron microscope confirmed that such structures are indeed aggregates (Figure 2c). For quantification, we took 2–4 mg of the 250–53 μm size fraction (both free and occluded), isolated all identifiable microaggregates contained therein, and weighed their amount. Aggregates were isolated from the size fraction using tweezers and referred to as isolated aggregates in this study. We acknowledge that our approach excludes other types of aggregates that may exist in soil, for example, sand grains with organic coatings. Yet, we decided to focus on such ideotypes of aggregates that are composed of a complexity of various binding units according to established theories on aggregate formation (summarized in Totsche et al., 2018).

2.3 | Bulk soil, soil fraction, and microaggregate C and $\delta^{13}\text{C}$ composition

We measured C content and $\delta^{13}\text{C}$ in bulk soil, free and occluded aggregate size fractions (250–53 μm), and composite samples of isolated free and occluded aggregates. Size fractions and bulk soil samples were milled before measurement. Isolated aggregate samples were not milled to avoid material loss and contamination. C content and $\delta^{13}\text{C}$ were measured with elemental analysis isotope ratio mass spectrometry (EA-IRMS) using a Delta S isotope ratio mass spectrometer (Finnigan MAT) coupled to an NA 1108 Elemental analyser (CE Instruments) via a ConFlo III interface (Finnigan MAT).

2.4 | LA-IRMS

LA-IRMS was used to investigate the small-scale variability of $\delta^{13}\text{C}$ within individual aggregates. We used manually isolated aggregates (see Section 2.2.) from the occluded 250–53 μm size fraction for this purpose. As LA-IRMS is very time-consuming, we performed such measurements only for the occluded aggregates and for three out of five samples from C3 and C4 soil. A small number of occluded aggregates per sample was embedded in water glass (liquid silica gel, reagent grade, Sigma-Aldrich) within a self-made teflon (PTFE) plate with cylindrical cavities of 1.5-mm depths and a diameter of 0.5 cm (Vergara Sosa et al., 2021). The water glass with embedded aggregates was dried at 60°C . Afterward, samples were collected from the PTFE cavities, stabilized in a ceramic ring, and polished using SiC abrasive paper (P1000, Buehler) to obtain cross-sections through aggregates (Figure 2d). Each sample contained three to four polished aggregates. Thus, we analyzed 11 individual aggregates from C4 soil and nine aggregates from C3 soil.

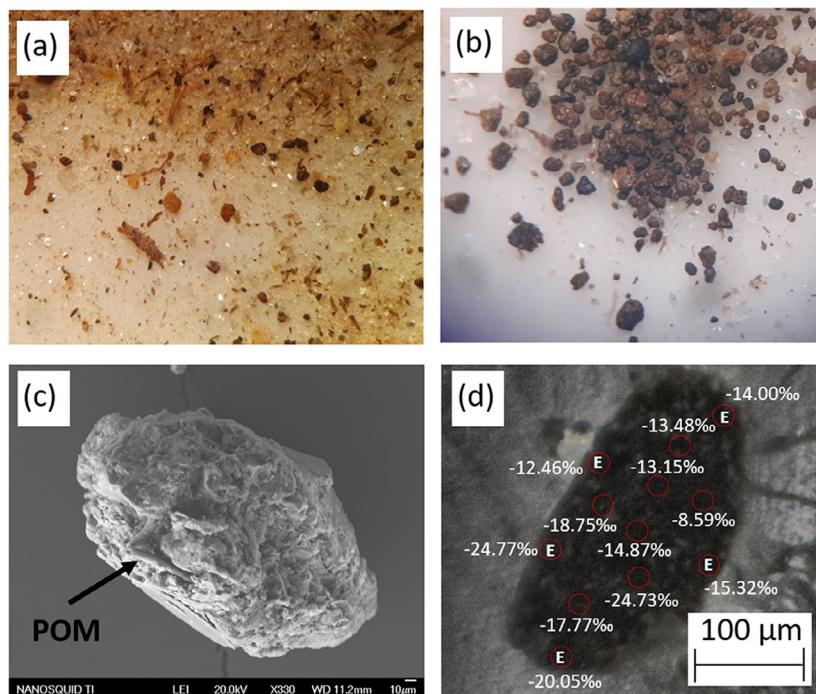


FIGURE 2 Aggregate isolation procedure, (a) after wet-sieving and ultrasound treatment of soil size fractions, (b) after isolation of hand-picked aggregates, (c) raster electron microscopy to confirm that the isolated structures are indeed aggregates (picture taken by N. Siebers; POM = particulate organic matter), (d) example for laser ablation-isotope ratio mass spectrometry measurements within one of the 20 measured aggregates. Sampling spots (20 µm) are indicated as red circles. The letter “E” indicates measurement spots that have been selected as exterior locations. Measurement spots free of soil organic carbon are not presented.

Cross sections were cleaned from abraded water glass using a brush and compressed air.

On each aggregate cross-section, 10–12 spots of 20-µm diameter were chosen for LA-IRMS measurements, half of them being located at the exterior of the aggregate and half of them at the interior (225 measurements in total, see Figure 2d for an example; all aggregates are presented in the Supporting Information Figure S1). Exterior was defined as the outer 20 µm of the cross-section, and interior locations had a distance of at least 20 µm to the surface. As some spots were free of C, that is, there was no difference in the peak area in comparison with the blank, the actually presented number of measurements was slightly lower (176 measurements).

For LA-IRMS measurements, we used a Teledyne LSX-213G2+ solid state Nd:YAG laser system (Teledyne LSX-213G2+, CETAC) coupled to a 900°C combustion oven, followed by two cryo-traps and a nafion trap for water (modified PreCon system) and an IRMS DeltaVplus with a ConFloIV interface (all from Thermo-Fisher Scientific; Rodionov et al., 2019).

The ablations were produced with spots of 20-µm size and 40 shots in 0.4-mL cell volume. Interferences by embedding (silica gel) were checked by sampling in the cell of the LA-IRMS system together with acryl as reference material (Rodionov et al., 2019). As reference, the in-house acryl standard was used (C content 60%; density 1.19 g cm⁻³; $\delta^{13}\text{C}_{\text{Acryl}} = -29.75 \pm 0.06\text{‰}$, relative to Vienna Pee Dee Belemnite (VPDB) using EA-IRMS). The CO₂ background in the sample cell was at 10.8 ± 0.4 mV, and the acryl reference was at $-29.75 \pm 0.20\text{‰}$.

A blank correction for isotope ratio measurement with small amounts of samples can be performed by regression or by subtraction (Ohlsson, 2013; Werner & Brand, 2001) and calculated as described by Werner et al. (1999) and Equation (1), where *A* is the area of the *m/z* 44

peak.

$$\delta^{13}\text{C}_{\text{sample}} = \frac{(\delta^{13}\text{C}_{\text{total}} \times A_{\text{total}} - \delta^{13}\text{C}_{\text{blank}} \times A_{\text{blank}})}{(A_{\text{total}} - A_{\text{blank}})} \quad (1)$$

2.5 | MRT calculation for SOC

To calculate MRT of SOC (in bulk soil, aggregate size fraction, isolated aggregates), we first calculated the proportion of newly incorporated C4-C based on Equation (2) where δ_{sample} is the $\delta^{13}\text{C}$ of the sample (bulk soil, isolated aggregates, or size fraction), δ_{control} is the $\delta^{13}\text{C}$ of the respective C3 control, and δ_{maize} is the average $\delta^{13}\text{C}$ of maize, which was assumed to be 12.2 according to Schiedung et al. (2017).

$$\text{Proportion of C4-derived C (\%)} = \frac{(\delta_{\text{sample}} - \delta_{\text{control}}) / (\delta_{\text{maize}} - \delta_{\text{control}})}{\times 100} \quad (2)$$

The proportion of C3-derived C was calculated by subtracting the proportion of C4-derived C from 100.

Subsequently, the rate constant of first-order decay (*k*) was calculated according to Equation (3), where *t* is the year of sampling, *t*₀ is the year where vegetation change from C3 to C4 was initiated, *C_t* is the remaining proportion of C3-C at the time of sampling (%), and *C_{t0}* the proportion of C3-C at *t*₀ (100%) for a simple 1-pool mixing model (Derrien & Amelung, 2011). The MRT was then calculated with Equation (3):

$$\text{MRT} = 1/k = -(t - t_0) / \ln(C_t / C_{t_0}) \quad (3)$$

2.6 | Statistics

We used analysis of variance (ANOVA) to investigate differences between fractions (i.e., size fraction, isolated aggregates, bulk soil) with sample ID (i.e., field replicate) as a block effect. ANOVA was carried

TABLE 1 Quantity, C content, and mean residence time (MRT) of bulk soil, aggregate size fractions, and isolated aggregates ($n = 5$ each).

		Proportion to bulk soil (%)	Proportion to size fraction (%)	C (%)	MRT of C in C4 soil (years)
C3	Bulk soil			1.22 ± 0.06^{ab}	
	Occluded size fraction	8.33 ± 1.72		0.84 ± 0.18^b	
	Isolated occluded aggr.	0.39 ± 0.06	4.84 ± 1.04	1.00 ± 0.49^b	
	Free size fraction	4.06 ± 1.33		1.65 ± 0.19^a	
	Isolated free aggregates	0.11 ± 0.05	2.73 ± 0.33	0.88 ± 0.19^b	
C4	Bulk soil			1.15 ± 0.07^a	57.8 ± 5.0^{ab}
	Occluded size fraction	5.57 ± 0.55		1.63 ± 0.05^a	35.4 ± 5.3^b
	Isolated occluded aggr.	0.19 ± 0.05	3.40 ± 0.56	1.90 ± 0.66^a	62.3 ± 25.6^{ab}
	Free size fraction	5.08 ± 1.23		1.84 ± 0.17^a	35.7 ± 2.4^b
	Isolated free aggregates	0.21 ± 0.03	4.23 ± 0.84	1.60 ± 0.51^a	105.0 ± 62.1^a

Note: Within each soil (C3, C4), different letters indicate significant differences ($p < 0.05$).

out separately for the three parameters of interest (C, MRT, and $\delta^{13}C$) and for each site (C3 and C4). The latter was necessary as a comparison between the two sites was not the scope of this study and because MRT could only be calculated for C4 soil. To investigate differences in $\delta^{13}C$ between interior and exterior locations of aggregates, ANOVA was performed for C3 and C4 soil separately with aggregate ID as block effect. Residuals were checked for normal distribution ($p > 0.001$) using the Shapiro test and for variance homogeneity with Levene's test. Tukey's post hoc test was used to investigate significant differences between fractions. Statistics were conducted in R (R Core Team, 2022).

3 | RESULTS

3.1 | Quantity and C content of aggregate fractions and isolated aggregates

The size fraction 250–53 μm had a weight contribution of 10%–14% to bulk soil, of which 40% on average occurred in the free fraction and 60% was occluded in macroaggregates (Table 1). Investigating the size fractions under a stereomicroscope revealed the presence of mineral particles, free POM, and aggregates (Figure 2a). Across both sites (C3 and C4 soil), the average proportion of isolated aggregates to the size fraction was $4.1\% \pm 1.1\%$ for occluded fractions and 3.5 ± 0.9 for free fractions. As a result, the proportion of occluded isolated aggregates (53–250 μm) to bulk soil was $0.29\% \pm 0.11\%$ and that of free aggregates was $0.16\% \pm 0.06\%$ (Table 1).

The C content of isolated occluded aggregates was, on average, higher than that of the respective size fraction, both in C3 and C4 soil. In contrast, the C content of isolated free aggregates was lower than that of the respective size fraction, both in C3 and C4 soil. Occluded aggregates had higher C contents than free aggregates. Yet, given large variations, these differences were not significant (Table 1).

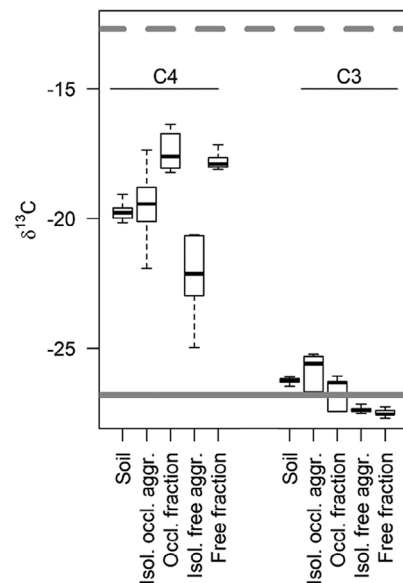


FIGURE 3 $\delta^{13}C$ of bulk soil, size fraction, and isolated aggregates in C4 soil and C3 soil. The gray solid line indicates the expected $\delta^{13}C$ of pure wheat litter (C3) and the dashed gray line the expected $\delta^{13}C$ of pure maize litter (C4) according to John et al. (2005). All boxes are based on $n = 5$ samples.

3.2 | Bulk composition of $\delta^{13}C$ in soil, size fractions, and soil aggregates and MRT of SOC

EA-IRMS measurements were conducted on homogenized bulk soil samples, size fractions, and isolated microaggregates from soil under C3 and soil under C3/C4 vegetation change.

In both C3 and C4 soil, the $\delta^{13}C$ values of isolated aggregates were less negative than those of the respective size fraction (Figure 3), with significant differences between isolated occluded aggregates and the occluded size fraction. Also, the free fraction and the isolated free aggregates had significantly more negative $\delta^{13}C$ values than occluded fractions and isolated occluded aggregates, respectively.

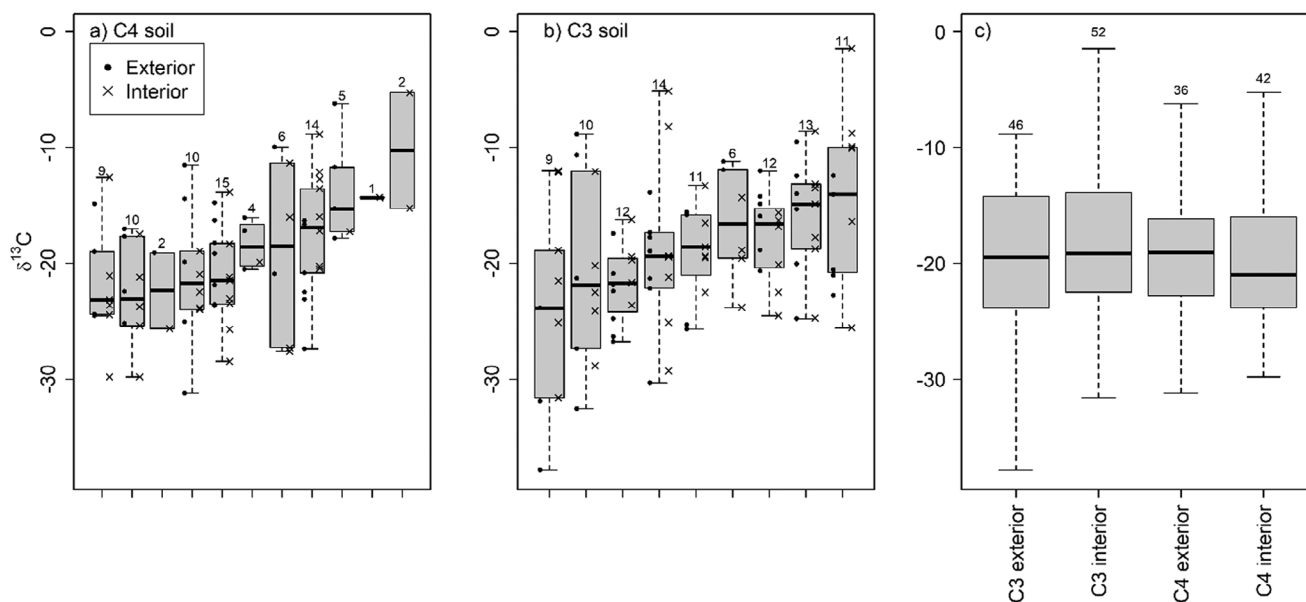


FIGURE 4 Range of $\delta^{13}\text{C}$ values in individual occluded microaggregates of (a) C4 soil and (b) C3 soil. Each box represents one individual aggregate. Aggregates are ordered according to their median $\delta^{13}\text{C}$ value. The number above the box indicates the total number of measurements within the aggregate. (c) Comparison of $\delta^{13}\text{C}$ between interior and exterior across all measured aggregates.

Using a 1-pool isotope mixing model using C3 and C4 plants as end members allowed for an estimation of MRT. It was considerably longer for the SOC of isolated aggregates than for the overall size fraction and the bulk soil (Table 1), suggesting that isolated microaggregates include primarily older, C3-derived SOC. This applied especially to free aggregates where differences between isolated aggregates and the respective size fraction were significant. SOC in occluded aggregates revealed only marginally and insignificantly longer residence times than in bulk soil.

3.3 | Microscale patterns of SOC turnover in soil microaggregates

The SOC turnover mechanisms were depicted from spatial microscale LA-IRMS analyses on isolated soil aggregates. The variability of $\delta^{13}\text{C}$ values within and also between individual aggregates was considerable, both in C4 (Figure 4a) and C3 soil (Figure 4b). There was no significant difference between C3 and C4 soil ($p = 0.41$). Also, there was no significant difference between the interior and exterior of aggregates ($p = 0.46$).

4 | DISCUSSION

4.1 | Recovery of “old” C3 material and “young” C4 material in bulk soil, size fractions, and isolated microaggregates after C3/C4 vegetation change

The bulk soil under maize was significantly more enriched in ^{13}C than the soil under C3 vegetation, indicating a contribution of C4-derived

material to SOM. Based on this, the calculated MRT of SOC in bulk soil was with 58 years in the range reported previously by Flessa et al. (2008) and John et al. (2005) for the respective field site. In the 250–53 μm occluded and free size fractions, this contribution of C4 material was considerably larger, evidenced by a less negative $\delta^{13}\text{C}$ value and thus resulting in lower calculated MRT, likely reflecting a considerable proportion of POM with rather short residence time in these size fractions (Besnard et al., 1996; Franzluebbers & Arshad, 1997; Figure 2a). Also, Poeplau et al. (2018) confirmed that POM is largely though not exclusively composed of C4-derived SOC at the same field site. Using a similar fractionation approach, John et al. (2005) calculated the MRT of the free 250–53 μm aggregate size fraction at the same field site and came to slightly longer MRTs of 60 years, which was comparable to bulk soil.

When aggregates were isolated from the size fractions, free POM was excluded. And indeed, isolated aggregates were significantly less enriched in ^{13}C than the respective size fraction, that is, they revealed more negative $\delta^{13}\text{C}$ values. This may point to a larger contribution of “old” C3 material to total carbon in isolated aggregates in comparison with size fractions. As a result, the MRT of SOC was longer in isolated aggregates than in the respective size fraction. The MRT of SOC in isolated aggregates also exceeded that of bulk soil, especially in the case of free aggregates. This seems to support earlier suggestions (Ladd et al., 1993) that microaggregation is an important physical stabilization mechanism for SOC. Yet, the proportion of isolated aggregates in size fractions was small (2.7%–4.8%). Considering that the size fraction 250–53 μm had already a small contribution to bulk soil in the here studied soil, the therefrom isolated aggregates had a negligible quantitative importance to bulk soil (0.1%–0.4%). As a result, microaggregates as those isolated in our study likely also have a minor impact on the bulk soil’s MRT.

Surprisingly, isolated free aggregates were less enriched in ^{13}C than isolated occluded aggregates. Hence, they seem to contain a larger proportion of “old” C3 material in comparison with isolated occluded aggregates. This questions the concept that macroaggregates increase the stability of occluded microaggregates (Six et al., 2004). The finding that SOC in occluded aggregates is not necessarily more protected than SOC in free aggregates appears reasonable as Plante et al. (2002) reported an MRT of SOC in macroaggregates ranging from 4 to 95 days. Puget et al. (2000) estimated that stable macroaggregates persist for a few years, pointing to high dynamics and little addition to the long-term protection of SOC by macroaggregates. Still, the fast turnover of macroaggregates does not explain our finding that isolated free aggregates contain even more of the old C3 material than isolated occluded aggregates. As macroaggregates form especially in the presence of roots (Amelung et al., 2023; Tisdall & Oades, 1982), they may be located in hot spots of microbial activity. This is also evidenced by larger C concentrations in isolated occluded than isolated free aggregates. Also, the $\delta^{13}\text{C}$ signature in C3 soil, where isolated occluded aggregates had less negative $\delta^{13}\text{C}$ values than isolated free aggregates, may point to a larger contribution of microbial-derived C in isolated occluded aggregates, which usually shows less negative $\delta^{13}\text{C}$ values than plant-derived C (Klink et al., 2022). As microbial activity fosters aggregate formation and stability (Abiven et al., 2007; Forster, 1990) but possibly also disruption, hot spots such as macroaggregates may therefore harbor comparatively young microaggregates.

4.2 | Small-scale patterns of $\delta^{13}\text{C}$ within individual microaggregates

When zooming into $\delta^{13}\text{C}$ patterns within individual aggregates, we expected that SOM located inside aggregates is older than that at the exterior. This may be the result of two processes: First, aggregates may form concentrically around a nucleus resulting in older SOC located at the interior. Second, microbes likely decompose SOM more rapidly at the exterior than the interior, given that inner aggregate pores are small and oxygen diffusion is likely limited (Amelung et al., 2002). This may result in a larger contribution of rather young microbial-derived C at the exterior. After C3/C4 change, older SOM in the interior may be indicated by a larger proportion of C3-derived SOM, compared with the aggregate's surface. In long-term C3 soil, this may be indicated by less negative $\delta^{13}\text{C}$ values at the exterior, compared with the interior, as microbial degradation, which is likely restricted inside an aggregate, is usually associated with ^{13}C enrichment (Gleixner et al., 1993; Menichetti et al., 2015). However, we did not find any significant differences in $\delta^{13}\text{C}$ values between interior and exterior locations in microaggregates, neither in C3 soil nor after C3/C4 vegetation change. Two processes may explain such findings. First, aggregates may repeatedly be disrupted and formed in soil (Six et al., 2000) and consequently do not exist in intact form for a long time. Such disruption and reformation may involve an entire breakdown and reformation or a partial reformation of subsections of microaggregates following temporal sequences of their formation, stabilization,

and turnover (Amelung et al., 2023; Schweizer et al., 2018; Vogel et al., 2014). This would obscure a systematically enhanced SOM turnover at the microaggregate exterior and result in a highly variable but unsystematic pattern as is the case in our study. Second, aggregates form at a distinct time point and are, as a whole, disconnected from microbial decay, that is, no spatial zonation develops. As the MRT of occluded aggregates was only marginally older than that of bulk soil and because we did not find an aggregate that consisted exclusively of “old” C3-derived SOC, we think that the first explanation is more likely. This leads to the conclusion that microaggregates do not persist in an intact form in such a long term that systematic differences in $\delta^{13}\text{C}$ patterns between exterior and interior parts can develop.

We also expected to find aggregates that contained only C3 material, that is, that formed before the vegetation change and were at least 36 years old. However, the variability of $\delta^{13}\text{C}$ values within individual aggregates was huge (Figure 4). On the one hand, we have to acknowledge that we only investigated 11 individual C4 aggregates, and some of them were so poor in C that only few locations could be characterized for natural ^{13}C abundance (for exact numbers, see Figure 4). Yet, at least we failed to detect aggregates that refrained from participating in SOC cycling during the last three decades. This, again, may indicate that microaggregates do not persist in an intact form in the long term, although this conclusion certainly needs to be considered with caution given the comparatively small number of measured aggregates.

4.3 | Limitation of carbon turnover time assessment on the microscale

Our interpretations of $\delta^{13}\text{C}$ variability in Section 4.2 require that the concept of source partitioning is valid on such a small spatial scale, that is, that simple isotope mixing between C3 and C4 plant-derived SOM can be applied to calculate MRT or to make assumptions about the source of SOM. Yet, differences in $\delta^{13}\text{C}$ values among individual SOM constituents (Amelung et al., 2008), the Suess effect (Friedli et al., 1986), microbial C fractionation processes (Werth & Kuzyakov, 2010), and preferential microbial utilization of substrates with different $\delta^{13}\text{C}$ signature (Blagodatskaya et al., 2011) may additionally contribute to variations of the $\delta^{13}\text{C}$ signal within a given microaggregate (for a recent review on the controls of $\delta^{13}\text{C}$ in soil, see Krüger et al., 2023). In principle, all these variations would average out if the same processes had a similar contribution in all 20- μm spots. In this case, differences in $\delta^{13}\text{C}$ between spots would result from different sources, that is, C3- or C4-derived SOM, which represents the basis for the source partitioning concept in larger scale approaches. Our spot size of 20 μm exceeds the size of many biological entities and mineral structures (Lehmann et al., 2008). Hence, the signal represents an average of diverse processes but those likely have a variable contribution to each spot. The large variability in C3 aggregates with only C3-derived SOM as carbon input demonstrates that small-scale variations in $\delta^{13}\text{C}$ at microaggregate level are largely driven by different decomposition stages of SOM or biological entities rather than solely by the primary (vegetation) source of C. Furthermore, the compositional spatial arrangement of

individual soil microaggregates and thus likely also their stable C isotope pattern have been found to be not reproducible (Lehndorff et al., 2021). Consequently, respective 20- μm spots within aggregates from C3 soil cannot necessarily be considered as a control for similar spots in C4 microaggregates. We conclude, therefore, that source partitioning and isotope mixing between C3 and C4 plant material for MRT calculation can only be applied when homogeneous background variations exist as it is likely the case in our homogenized bulk soil samples, composite samples of size fractions, and composite samples of isolated aggregates. Yet, it does not exist in microscale resolution, thus significantly affecting the accuracy of the in soil science established method for MRT assessment at the microscale. Interpretations based on micro-spatial variability of $\delta^{13}\text{C}$ inside microaggregates thus require an update of source mixing models toward microbial process understanding and likely a deviation from simple 1-pool concepts as already indicated by Derrien and Amelung (2011) and Klink et al. (2022).

When comparing microscale results (LA-IRMS) with those obtained from composite samples of isolated aggregates (EA-IRMS), we found an immense offset in $\delta^{13}\text{C}$. The most surprising finding in this context was that $\delta^{13}\text{C}$ values of isolated C3 aggregates differed significantly from C4 aggregates when composite samples of several isolated aggregates were measured (Figure 3) but not when small spots of 20 μm within individual aggregates were measured (Figure 4). Especially aggregates from C3 soil were found to be more ^{13}C -enriched when small spots were measured with LA-IRMS in comparison with composite samples measured with EA-IRMS. We suspect that the small-scale measurements within individual aggregates do not necessarily reflect the mean $\delta^{13}\text{C}$ of entire aggregates because what we most often shoot at with the LA-IRMS is not necessarily the SOC that dominates the total C and total $\delta^{13}\text{C}$ of the aggregate. Spots with high C content, such as occluded POM, may quantitatively dominate the mean $\delta^{13}\text{C}$ when composite samples of isolated aggregates are measured. Yet, those cover only a small area of an aggregate cross-section (Lehndorff et al., 2021) and are therefore only eventually hit by the laser beam. Hence, it is more likely that LA-IRMS measurements are conducted at locations free of POM, that is, at locations where C-poor materials dominate that are quantitatively not relevant for the aggregates mean $\delta^{13}\text{C}$ despite a large spatial coverage. With clay minerals being an important building unit of aggregates (Totsche et al., 2018), such C-poor materials could be mineral-associated organic matter, which has been found to be dominated by microbial residues (e.g., Klink et al., 2022). These mineral-associated microbial residues were reported to be enriched in $\delta^{13}\text{C}$ in comparison with bulk soil and POM (Klink et al., 2022; Kohl et al., 2015). For instance, saprotrophic fungi contributed with a $\delta^{13}\text{C}$ value of -22‰ to a bulk soil having a $\delta^{13}\text{C}$ of -26.5‰ , while POM was with $\delta^{13}\text{C}$ of -27.5‰ even more depleted in ^{13}C (Klink et al., 2022). The order of magnitude between these reported $\delta^{13}\text{C}$ values is similar to the observed offset between the composite and the spatially resolved approach for $\delta^{13}\text{C}$ analyses used in our study. We think that this mismatch between measured $\delta^{13}\text{C}$ at small spots and $\delta^{13}\text{C}$ of complete aggregates highlights a new challenge that is needed to address for understanding the source and turnover time of OM in soil aggregates.

5 | CONCLUSION

Isolated aggregates stored older SOM than size fractions and bulk soil. Yet, they had a small quantitative contribution to bulk soil. Also, we failed to detect systematic gradients in natural ^{13}C abundance between aggregate exterior and interior. Hence, our data question a radial formation and disruption of aggregates with SOC being especially protected in their interior. Our data rather point to a regular formation and disruption of aggregates, which does not occur concentrically but because of coagulation and breaking up of primary building blocks.

The large and random spatial variability of $\delta^{13}\text{C}$ values across and within aggregates challenges the applicability of the simple concept for source partitioning at the microscale. Microbial transformation and decay rather than source mixing seem to dominate the small-scale distribution of $\delta^{13}\text{C}$. The assessment of stable C isotope ratios in undisturbed microstructures will be valuable to study C exchange and turnover processes in biological tissues such as plants, in organo-mineral associations in different environments, and in temporal or environmental gradients such as microscale accumulation layers or environmental interfaces such as between root and soil. As a next step toward SOC turnover understanding, we propose to gain a systematic overview about small-scale C isotope ratios of plant residues and microbial residues to relate the observed heterogeneity to processes. This will certainly include the involvement of higher-resolution techniques and environmental microbiology. Finally, our results warn against drawing conclusions about aggregate dynamics based on size fractions, as those contain besides a small proportion of aggregates especially free POM and mineral particles that may dominate the outcome.

ACKNOWLEDGMENTS

We thank Henri Braunmiller, Max Frank, Friederike Dellmann, and Leoni Koch for their help with aggregate isolation, Nina Siebers for conducting raster electron microscopy and providing Figure 2c, Gerhard Gebauer (BayCEER—Laboratory of Isotope Biogeochemistry, Bayreuth) for conducting $\delta^{13}\text{C}$ measurements, and the German Research Foundation for funding (DFG Am 134/25/2 and project number 251268514).

Open access funding enabled and organized by Projekt DEAL.

DATA AVAILABILITY STATEMENT

The data that support the findings of this study are available from the corresponding author upon reasonable request.

ORCID

Jacqueline Kaldun  <https://orcid.org/0000-0003-4510-2732>

Wulf Amelung  <https://orcid.org/0000-0002-4920-4667>

REFERENCES

- Abiven, S., Menasseri, S., Angers, D. A., & Leterme, P. (2007). Dynamics of aggregate stability and biological binding agents during decomposition of organic materials. *European Journal of Soil Science*, 58(1), 239–247.

- Amelung, W., Meyer, N., Rodionov, A., Knief, C., Aehnelt, M., Bauke, S. L., Biesgen, D., Dultz, S., Guggenberger, G., Jaber, M., Klumpp, E., Kögel-Knabner, I., Nischwitz, V., Schweizer, S. A., Wu, B., Totsche, K. U., & Lehndorff, E. (2023). Process sequence of soil aggregate formation disentangled through multi-isotope labelling. *Geoderma*, 429, 116226. <https://doi.org/10.1016/j.geoderma.2022.116226>
- Amelung, W., Brodowski, S., Sandhage-Hofmann, A., & Bol, R. (2008). Combining biomarker with stable isotope analyses for assessing the transformation and turnover of soil organic matter. *Advances in Agronomy*, 100, 155–250.
- Amelung, W., Kaiser, K., Kammerer, G., & Sauer, G. (2002). Organic carbon at soil particle surfaces—Evidence from x-ray photoelectron spectroscopy and surface abrasion. *Soil Science Society of America Journal*, 66(5), 1526–1530.
- Amelung, W., & Zech, W. (1996). Organic species in ped surface and core fractions along a climosequence in the prairie, North America. *Geoderma*, 74(3-4), 193–206.
- Balesdent, J., & Mariotti, A. (1996). Measurement of soil organic matter turnover using ^{13}C natural abundance. In T. W. Boutton & S. Yamasaki (Eds.), *Mass spectrometry of soils* (pp. 83–112). Marcel Dekker.
- Balesdent, J., Besnard, E., Arrouays, D., & Chenu, C. (1998). The dynamics of carbon in particle-size fractions of soil in a forest-cultivation sequence. *Plant and Soil*, 201, 49–57.
- Besnard, E., Chenu, C., Balesdent, J., Puget, P., & Arrouays, D. (1996). Fate of particulate organic matter in soil aggregates during cultivation. *European Journal of Soil Science*, 47(4), 495–503.
- Blagodatskaya, E., Yuyukina, T., Blagodatsky, S., & Kuzyakov, Y. (2011). Turnover of soil organic matter and of microbial biomass under C3–C4 vegetation change: Consideration of ^{13}C fractionation and preferential substrate utilization. *Soil Biology and Biochemistry*, 43(1), 159–166.
- Bucka, F. B., Kölbl, A., Uteu, D., Peth, S., & Kögel-Knabner, I. (2019). Organic matter input determines structure development and aggregate formation in artificial soils. *Geoderma*, 354, 113881. <https://doi.org/10.1016/j.geoderma.2019.113881>
- Burger, D. J., Bauke, S. L., Amelung, W., & Sommer, M. (2023). Fast agricultural topsoil re-formation after complete topsoil loss—Evidence from a unique historical field experiment. *Geoderma*, 434, 116492. <https://doi.org/10.1016/j.geoderma.2023.116492>
- Buyanovsky, G. A., Aslam, M., & Wagner, G. H. (1994). Carbon turnover in soil physical fractions. *Soil Science Society of America Journal*, 58(4), 1167–1173.
- Derrien, D., & Amelung, W. (2011). Computing the mean residence time of soil carbon fractions using stable isotopes: Impacts of the model framework. *European Journal of Soil Science*, 62(2), 237–252.
- Elliott, E. T., Palm, C. A., Reuss, D. E., & Monz, C. A. (1991). Organic matter contained in soil aggregates from a tropical chronosequence: Correction for sand and light fraction. *Agriculture, Ecosystems & Environment*, 34(1-4), 443–451.
- Elliott, E. T. (1986). Aggregate structure and carbon, nitrogen, and phosphorus in native and cultivated soils. *Soil Science Society of America Journal*, 50(3), 627–633.
- Fernandez, I., Mahieu, N., & Cadisch, G. (2003). Carbon isotopic fractionation during decomposition of plant materials of different quality. *Global Biogeochemical Cycles*, 17(3). <https://doi.org/10.1029/2001GB001834>
- Flessa, H., Amelung, W., Helfrich, M., Wiesenberger, G. L., Gleixner, G., Brodowski, S., Rethemeyer, J., Kramer, C., & Grootes, P. M. (2008). Storage and stability of organic matter and fossil carbon in a Luvisol and Phaeozem with continuous maize cropping: A synthesis. *Journal of Plant Nutrition and Soil Science*, 171(1), 36–51.
- Forster, S. M. (1990). The role of microorganisms in aggregate formation and soil stabilization: Types of aggregation. *Arid Land Research and Management*, 4(2), 85–98.
- Foster, R. (1988). Microenvironments of soil microorganisms. *Biology and Fertility of Soils*, 6, 189–203.
- Franzluebbers, A. J., & Arshad, M. A. (1997). Particulate organic carbon content and potential mineralization as affected by tillage and texture. *Soil Science Society of America Journal*, 61(5), 1382–1386.
- Friedli, H., Lötscher, H., Oeschger, H., Siegenthaler, U., & Stauffer, B. (1986). Ice core record of the $^{13}\text{C}/^{12}\text{C}$ ratio of atmospheric CO_2 in the past two centuries. *Nature*, 324(6094), 237–238.
- Gleixner, G., Poirier, N., Bol, R., & Balesdent, J. (2002). Molecular dynamics of organic matter in a cultivated soil. *Organic Geochemistry*, 33(3), 357–366.
- Gleixner, G., Danier, H. J., Werner, R. A., & Schmidt, H. L. (1993). Correlations between the ^{13}C content of primary and secondary plant products in different cell compartments and that in decomposing Basidiomycetes. *Plant Physiology*, 102(4), 1287–1290.
- Jastrow, J. D. (1996). Soil aggregate formation and the accrual of particulate and mineral-associated organic matter. *Soil Biology and Biochemistry*, 28(4-5), 665–676.
- Jenkinson, D. S. (1990). The turnover of organic carbon and nitrogen in soil. *Philosophical Transactions of the Royal Society of London. Series B: Biological Sciences*, 329(1255), 361–368.
- Jiang, X., Wright, A. L., Wang, J., & Li, Z. (2011). Long-term tillage effects on the distribution patterns of microbial biomass and activities within soil aggregates. *Catena*, 87(2), 276–280.
- John, B., Yamashita, T., Ludwig, B., & Flessa, H. (2005). Storage of organic carbon in aggregate and density fractions of silty soils under different types of land use. *Geoderma*, 128(1-2), 63–79.
- Klink, S., Keller, A. B., Wild, A. J., Baumert, V. L., Gube, M., Lehndorff, E., Meyer, N., Mueller, C. W., Phillips, R. P., & Pausch, J. (2022). Stable isotopes reveal that fungal residues contribute more to mineral-associated organic matter pools than plant residues. *Soil Biology and Biochemistry*, 168, 108634. <https://doi.org/10.1016/j.soilbio.2022.108634>
- Kohl, L., Laganière, J., Edwards, K. A., Billings, S. A., Morrill, P. L., Van Biesen, G., & Ziegler, S. E. (2015). Distinct fungal and bacterial $\delta^{13}\text{C}$ signatures as potential drivers of increasing $\delta^{13}\text{C}$ of soil organic matter with depth. *Biogeochemistry*, 124, 13–26.
- Krause, L., Rodionov, A., Schweizer, S. A., Siebers, N., Lehndorff, E., Klumpp, E., & Amelung, W. (2018). Microaggregate stability and storage of organic carbon is affected by clay content in arable Luvisols. *Soil and Tillage Research*, 182, 123–129.
- Krüger, N., Finn, D. R., & Don, A. (2023). Soil depth gradients of organic carbon-13—A review on drivers and processes. Plant and Soil. Advance online publication. <https://doi.org/10.1007/s11104-023-06328-5>
- Ladd, J. N., Foster, R. C., & Skjemstad, J. O. (1993). Soil structure: Carbon and nitrogen metabolism. In L. Brussaard & M. J. Kooistra (Eds.), *Soil structure/soil biota interrelationships* (pp. 401–434). Elsevier.
- Lehmann, J., Solomon, D., Kinyangi, J., Dathé, L., Wirick, S., & Jacobsen, C. (2008). Spatial complexity of soil organic matter forms at nanometre scales. *Nature Geoscience*, 1(4), 238–242.
- Lehndorff, E., Rodionov, A., Plümer, L., Rottmann, P., Spiering, B., Dultz, S., & Amelung, W. (2021). Spatial organization of soil microaggregates. *Geoderma*, 386, 114915. <https://doi.org/10.1016/j.geoderma.2020.114915>
- Lobe, I., Sandhage-Hofmann, A., Brodowski, S., Du Preez, C. C., & Amelung, W. (2011). Aggregate dynamics and associated soil organic matter contents as influenced by prolonged arable cropping in the South African Highveld. *Geoderma*, 162(3-4), 251–259.
- Menichetti, L., Houot, S., van Oort, F., Kätterer, T., Christensen, B. T., Chenu, C., Barré, P., Vasilyeva, N. A., & Ekblad, A. (2015). Increase in soil stable carbon isotope ratio relates to loss of organic carbon: results from five long-term bare fallow experiments. *Oecologia*, 177, 811–821.
- Moni, C., Derrien, D., Hatton, P. J., Zeller, B., & Kleber, M. (2012). Density fractions versus size separates: Does physical fractionation isolate functional soil compartments? *Biogeosciences*, 9(12), 5181–5197.
- Monreal, C. M., Schulten, H. R., & Kodama, H. (1997). Age, turnover and molecular diversity of soil organic matter in aggregates of a Gleysol. *Canadian Journal of Soil Science*, 77(3), 379–388.

- Ohlsson, K. A. (2013). Uncertainty of blank correction in isotope ratio measurement. *Analytical Chemistry*, 85(11), 5326–5329.
- Plante, A. F., Feng, Y., & McGill, W. B. (2002). A modeling approach to quantifying soil macroaggregate dynamics. *Canadian Journal of Soil Science*, 82(2), 181–190.
- Poeplau, C., Don, A., Six, J., Kaiser, M., Benbi, D., Chenu, C., Cotrufo, M. F., Derrien, D., Gioacchini, P., Grand, S., Gregorich, E., Griepentrog, M., Gunina, A., Haddix, M., Kuzyakov, Y., Kühnel, A., Macdonald, L. M., Soong, J., Trigalet, S., ... Nieder, R. (2018). Isolating organic carbon fractions with varying turnover rates in temperate agricultural soils—A comprehensive method comparison. *Soil Biology and Biochemistry*, 125, 10–26.
- Puget, P., Chenu, C., & Balesdent, J. (2000). Dynamics of soil organic matter associated with particle-size fractions of water-stable aggregates. *European Journal of Soil Science*, 51(4), 595–605.
- R Core Team. (2022). *R: A language and environment for statistical computing*. R Foundation for Statistical Computing. <https://www.R-project.org/>
- Rabbi, S. M. F., Hua, Q., Daniel, H., Lockwood, P. V., Wilson, B. R., & Young, I. M. (2013). Mean residence time of soil organic carbon in aggregates under contrasting land uses based on radiocarbon measurements. *Radiocarbon*, 55(1), 127–139.
- Rodionov, A., Lehdorff, E., Stremtan, C. C., Brand, W. A., Königshoven, H.-P., & Amelung, W. (2019). Spatial microanalysis of natural $^{13}\text{C}/^{12}\text{C}$ abundance in environmental samples using laser ablation-isotope ratio mass spectrometry. *Analytical Chemistry*, 91(9), 6225–6232.
- Schiedung, H., Tilly, N., Hütt, C., Welp, G., Brüggemann, N., & Amelung, W. (2017). Spatial controls of topsoil and subsoil organic carbon turnover under C3–C4 vegetation change. *Geoderma*, 303, 44–51.
- Schweizer, S. A., Hoeschen, C., Schlüter, S., Kögel-Knabner, I., & Mueller, C. W. (2018). Rapid soil formation after glacial retreat shaped by spatial patterns of organic matter accrual in microaggregates. *Global Change Biology*, 24(4), 1637–1650.
- Sexstone, A. J., Revsbech, N. P., Parkin, T. B., & Tiedje, J. M. (1985). Direct measurement of oxygen profiles and denitrification rates in soil aggregates. *Soil Science Society of America Journal*, 49(3), 645–651.
- Shrestha, B. M., Sitaula, B. K., Singh, B. R., & Bajracharya, R. M. (2004). Soil organic carbon stocks in soil aggregates under different land use systems in Nepal. *Nutrient Cycling in Agroecosystems*, 70, 201–213.
- Siebers, N., Abdelrahman, H., Krause, L., & Amelung, W. (2018). Bias in aggregate geometry and properties after disintegration and drying procedures. *Geoderma*, 313, 163–171.
- Six, J., Bossuyt, H., Degryze, S., & Denef, K. (2004). A history of research on the link between (micro) aggregates, soil biota, and soil organic matter dynamics. *Soil and Tillage Research*, 79(1), 7–31.
- Six, J., Elliott, E. T., & Paustian, K. (2000). Soil macroaggregate turnover and microaggregate formation: A mechanism for C sequestration under no-tillage agriculture. *Soil Biology and Biochemistry*, 32(14), 2099–2103.
- Tisdall, J. M., & Oades, J. M. (1982). Organic matter and water-stable aggregates in soils. *Journal of Soil Science*, 33(2), 141–163.
- Totsche, K. U., Amelung, W., Gerzabek, M. H., Guggenberger, G., Klumpp, E., Knief, C., Lehdorff, E., Mikutta, R., Peth, S., Prechtel, A., Ray, N., & Kögel-Knabner, I. (2018). Microaggregates in soils. *Journal of Plant Nutrition and Soil Science*, 181(1), 104–136.
- Vergara Sosa, M., Lehdorff, E., Rodionov, A., Gocke, M., Sandhage-Hofmann, A., & Amelung, W. (2021). Micro-scale resolution of carbon turnover in soil—Insights from laser ablation isotope ratio mass spectrometry on water-glass embedded aggregates. *Soil Biology and Biochemistry*, 159, 108279. <https://doi.org/10.1016/j.soilbio.2021.108279>
- Vogel, C., Mueller, C. W., Hoeschen, C., Buegger, F., Heister, K., Schulz, S., Schloter, M., & Kögel-Knabner, I. (2014). Submicron structures provide preferential spots for carbon and nitrogen sequestration in soils. *Nature Communications*, 5(1), 2947. <https://doi.org/10.1038/ncomms3947>
- Waters, A. G., & Oades, J. M. (1991). Organic matter in water-stable aggregates. In W. S. Wilson (Ed.), *Advances in Soil Organic Matter Research: The Impact on Agriculture and the Environment* (Vol. 90, pp. 163–174). Woodhead Publishing.
- Werner, R. A., & Brand, W. A. (2001). Referencing strategies and techniques in stable isotope ratio analysis. *Rapid Communications in Mass Spectrometry*, 15(7), 501–519.
- Werner, R. A., Bruch, B. A., & Brand, W. A. (1999). ConFlo III—An interface for high precision $\delta^{13}\text{C}$ and $\delta^{15}\text{N}$ analysis with an extended dynamic range. *Rapid Communications in Mass Spectrometry*, 13(13), 1237–1241.
- Werth, M., & Kuzyakov, Y. (2010). ^{13}C fractionation at the root-microorganisms-soil interface: A review and outlook for partitioning studies. *Soil Biology and Biochemistry*, 42(9), 1372–1384.

SUPPORTING INFORMATION

Additional supporting information can be found online in the Supporting Information section at the end of this article.

How to cite this article: Meyer, N., Kaldun, J., Rodionov, A., Amelung, W., & Lehdorff, E. (2024). Turnover of soil microaggregate-protected carbon and the challenge of microscale analyses. *Journal of Plant Nutrition and Soil Science*, 187, 143–152. <https://doi.org/10.1002/jpln.202300154>